Weierstraß-Institut
für Angewandte Analysis und Stochastik

im Forschungsverbund Berlin e.V.

Preprint ISSN 0946 – 8633

Stochastic Weighted Particle Method – Theory and Numerical Examples

Sergej Rjasanow [1] and Wolfgang Wagner[2]

submitted: 4th April 2005

[1] Fachrichtung 6.1 – Mathematik
Universität des Saarlandes
Postfach 15 11 50
66041 Saarbrücken, Germany
E-Mail: rjasanow@num.uni-sb.de

[2] Weierstrass Institute for
Applied Analysis and Stochastics
Mohrenstrasse 39
10117 Berlin, Germany
E-Mail: wagner@wias-berlin.de

No. 1021
Berlin 2005

2000 *Mathematics Subject Classification.* 65C05, 82C80.

Key words and phrases. Boltzmann equation, Stochastic numerics, Variance reduction.

Edited by
Weierstraß-Institut für Angewandte Analysis und Stochastik (WIAS)
Mohrenstraße 39
10117 Berlin
Germany

Fax: + 49 30 2044975
E-Mail: preprint@wias-berlin.de
World Wide Web: http://www.wias-berlin.de/

Abstract

In the present paper we give a theoretical background of the Stochastic Weighted Particle Method (SWPM) for the classical Boltzmann equation. This numerical method was developed for problems with big deviation in magnitude of values of interest. We describe the corresponding algorithms, give a brief summary of the convergence theory and illustrate the new possibilities by numerical tests.

Contents

1 Introduction **2**

2 Description of the SWPM **3**
2.1 The Algorithm 3
2.2 Examples of the SWPM 8
2.3 Reduction of Particles 10
2.4 Theoretical Foundation and Convergence 13

3 Numerical examples and tests **16**
3.1 Statistical notions 16
3.2 Spatially homogeneous Boltzmann Equation 17
3.3 Spatially 2-dimensional Boltzmann Equation 23

References **31**

1 Introduction

The object of our considerations is the classical Boltzmann equation for a monoatomic, dilute gas

$$\frac{\partial}{\partial t} f + (v, \mathrm{grad}_x f) = Q(f,f) \tag{1}$$

which describes the time evolution of the particle density

$$f = f(t,x,v): \ \mathbb{R}_+ \times \Omega \times \mathbb{R}^3 \to \mathbb{R}_+ .$$

Here $\mathbb{R}_+$ denotes the set of non-negative real numbers and $\Omega \subset \mathbb{R}^3$ is a domain in physical space. The right-hand side of the equation (1), known as the collision integral or the collision term, is of the form

$$Q(f,f)(v) = \int\limits_{\mathbb{R}^3} \int\limits_{S^2} B(v,w,e)\Big(f(v')f(w') - f(v)f(w)\Big)\, de\, dw \,. \tag{2}$$

Note that $Q(f,f)$ depends on t and x only as parameters, so we have omitted this dependence and written (2) in order not to overload the formulae. The following notations have been used in (2): $v,w \in \mathbb{R}^3$ are the pre-collision velocities, $e \in S^2 \subset \mathbb{R}^3$ is a unit vector, $v',w' \in \mathbb{R}^3$ are the post-collision velocities and $B(v,w,e)$ is the collision kernel. The operator $Q(f,f)$ represents the change of the distribution function $f(t,x,v)$ due to the binary collisions between particles. A single collision results in the change of the velocities of the colliding partners

$$v,w \ \to v',w' \,. \tag{3}$$

The collision transformation (3) conserves the momentum and the energy

$$v + w = v' + w', \ |v|^2 + |w|^2 = |v'|^2 + |w'|^2 \tag{4}$$

and can be written in the following form

$$v' = \frac{1}{2}(v + w + |u|e), \ w' = \frac{1}{2}(v + w - |u|e) \,, \ e \in S^2 \,, \tag{5}$$

where $u = v - w$ denotes the relative velocity of the colliding particles. We will deal with the following classical models for the collision kernel $B(v,w,e)$. The particles of the hard spheres model are assumed to be the ideally elastic balls. The corresponding collision kernel takes the form

$$B(v,w,e) = \frac{1}{4\sqrt{2}\,\pi\, Kn}\,|u| \tag{6}$$

where Kn denotes the dimensionless Knudsen number. We will also consider the collision kernel of the form

$$B(v,w,e) = \frac{1}{4\,\pi} \tag{7}$$

which corresponds to the Maxwell molecules. The Boltzmann equation (1) is subjected to an initial condition

$$f(0, x, v) = f_0(x, v), \; x \in \Omega, \; v \in \mathbb{R}^3$$

and to the boundary conditions on $\Gamma = \partial\Omega$. If the domain under consideration is unbounded we have to pose an additional condition at infinity

$$f(t, x, v) \to f_\infty(t, v) \text{ for } |x| \to \infty . \tag{8}$$

In this paper we apply the Stochastic Weighted Particle Method (SWPM) to the numerical solution of the Boltzmann equation (1). This method was introduced in [RW96b], where we presented first numerical results for the one-dimensional heat exchange problem. The convergence of the method was investigated in [RW98], where we were also able to show a drastic reduction of the stochastic fluctuations using the SWPM for one model kinetic equation. In [RW96a] we presented a detailed study of different effects of the numerical solution of this equation. The computation of the macroscopic quantities in the regions with low particle density was of special interest. In [RSW98] the reduction of particles was investigated. The SWPM was applied to the numerical solution of the spatially two-dimensional Boltzmann equation in [RW01]. The main difference between the SWPM and other particle schemes for the Boltzmann equation [Bir94], [NGS91], [IR89] is the idea of a random weight transfer between particles during collisions.

The paper is organised as follows. In Section 2. we describe the SWPM procedure, give two examples for the reduction of particles and formulate the convergence theorem. Some numerical examples for spatially homogeneous and for spatially two-dimensional Boltzmann equation will be presented in Section 3. Finally we draw some conclusions.

2 Description of the SWPM

2.1 The Algorithm

The main idea of all particle methods for the Boltzmann equation (1) is an approximation of the sequence of measures

$$f(t_k, x, v)dxdv \, , \; t_k = k\,\Delta t \, , \; k = 0, 1, \dots \, , \; \Delta t > 0 \, ,$$

by a sequence of point measures

$$\mu(t_k, dx, dv) = \sum_{j=1}^{n(t_k)} g_j(t_k) \delta_{\left(x_j(t_k), \, v_j(t_k)\right)}(dx, dv) \, , \quad k = 0, 1, \dots \, , \tag{9}$$

defined by the families of particles

$$\Big(g_j(t_k), x_j(t_k), v_j(t_k) \Big)_{j=1}^{n(t_k)} , \; k = 0, 1, \dots \; . \tag{10}$$

The behaviour of the system (10) can be described as follows. The first step ($k = 0$) is an approximation of the initial measure

$$f_0(x, v)dxdv$$

by a system of particles (10) for $t_0 = 0$. Usually, one uses constant weights

$$g_j(0) = g\,,\ j = 1, ..., n(0).$$

Then the particles move according to their velocities, i.e.

$$x_j(t) = x_j(t_k) + (t - t_k)v_j(t_k)\,,\ t \in [t_k, t_{k+1}]\,.$$

If a particle crosses the "outflow boundary" during this step then this particle will be removed from the further simulation. The velocity of a particle changes according to the boundary condition if this particle hits the "boundary of the body". Then the particle continues its motion with a new velocity for the rest of the time interval. The weights of particles remain the same during this "free flow step". Through the "inflow boundary" new particles enter the computational domain. The "collision step" can be described as follows. First, all particles are sorted in the spatial cells $\Omega_\ell\,,\ \ell = 1, ..., N_c$. These cells define a non-overlapping decomposition of the computational domain

$$\Omega = \bigcup_{\ell=1}^{N_c} \Omega_\ell\,.$$

In each cell $\Omega_\ell,\ \ell = 1, ..., N_c$, collisions of $n_\ell(t_k)$ particles are simulated. This is the most crucial part of the whole procedure. Here we also have the main difference between the SWPM and other particle methods which use constant weights. The collision simulation step in one spatial cell $\Omega_\ell,\ \ell = 1, \ldots, N_c$, corresponds to the mollified equation [CIP94]

$$\frac{\partial f}{\partial t}(t, x, v) = \int\limits_{\Omega}\int\limits_{\mathbb{R}^3}\int\limits_{S^2} h_\ell(x, y)B(v, w, e)\Big(f(x, v')f(y, w') - f(x, v)f(y, w)\Big)\, de\, dw\, dy\,,$$

where

$$h_\ell(x, y) \quad = \quad \frac{1}{|\Omega_\ell|}\chi_{\Omega_\ell}(x)\chi_{\Omega_\ell}(y)\,, \tag{11}$$

is a spatial mollifier, $|\Omega_\ell|$ denotes the volume of the cell Ω_ℓ and $\chi_{\Omega_\ell}(x)$ is the indicator function of the set Ω_ℓ.

The stochastic process of the collisions is

$$Z(t) = \{(g_j(t), x_j(t), v_j(t))\,,\ j = 1, ..., n\}\,, \quad t \geq t_k\,. \tag{12}$$

Here we now use the local numbering of particles in the cell Ω_ℓ and denote $n = n_\ell(t_k)$. Let $\mathcal{Z}$ be the state space of the process (12), i.e. the union of all possible particles systems of the form (10). The infinitesimal generator of the process (12) is given by

$$\mathcal{A}(\Phi)(z) = \int_{\mathcal{Z}} \Big(\Phi(\tilde{z}) - \Phi(z)\Big)\, Q(z; d\tilde{z}) \tag{13}$$

where Q denotes the transition measure

$$Q(z; d\tilde{z}) = \frac{1}{2} \sum_{1 \le i \ne j \le n} \int_{S^2} \delta_{J(z;i,j,e)}\, q(z;i,j,e)\, de\,, \tag{14}$$

Φ is a measurable function of the argument

$$z = ((g_1, x_1, v_1), \ldots, (g_n, x_n, v_n))$$

and

$$\Big(J(z;i,j,e)\Big)_k = \begin{cases} (g_k, x_k, v_k) & \text{, if} \quad k \le n\,,\ k \ne i, j\,, \\ (g_i - G(z;i,j,e), x_i, v_i)) & \text{, if} \quad k = i\,, \\ (g_j - G(z;i,j,e), x_j, v_j) & \text{, if} \quad k = j\,, \\ (G(z;i,j,e), x_i, v_i') & \text{, if} \quad k = n+1\,, \\ (G(z;i,j,e), x_j, v_j') & \text{, if} \quad k = n+2\,, \end{cases} \tag{15}$$

where v_i', v_j' are defined as in (5). The function $G(z;i,j,e)$ is called "weight transfer function". This function, the intensity kernel $q(z;i,j,e)$ of the generator (13) and the collision kernel of the Boltzmann equation (1) are connected via the basic relationship

$$q(z;i,j,e)\, G(z;i,j,e) = h_\ell(x_i, x_j)\, B(v_i, v_j, e)\, g_i\, g_j \tag{16}$$

which has been proved [RW96a] to be sufficient for the convergence of the method. The behaviour of the process (12) is as follows: The waiting time $\hat{\tau}(z)$ between process jumps can be defined either as a random variable with the distribution

$$\text{Prob}\,\{\hat{\tau}(z) \ge t\} \;=\; \exp(-\hat{\pi}(z)\, t)\,,$$

where

$$\hat{\pi}(z) \;=\; \frac{1}{2} \sum_{1 \le i \ne j \le n} \hat{q}_{max}(z;i,j) \tag{17}$$

and

$$\int_{S^2} q(z;i,j,e)\, de \;\le\; \hat{q}_{max}(z;i,j)\,. \tag{18}$$

or as a deterministic object by

$$\hat{\tau}(z) = \hat{\pi}(z)^{-1}. \tag{19}$$

Then the collision partners (i.e. the indices i and j) must be chosen. The distribution of the parameters i and j is determined by the probabilities

$$\frac{\hat{q}_{max}(z;i,j)}{\sum_{1\le i\ne j\le n}\hat{q}_{max}(z;i,j)}. \tag{20}$$

For given i and j, the jump is fictitious with probability

$$1-\frac{\int\limits_{S^2} q(z;i,j,e)\,de}{\hat{q}_{max}(z;i,j)}. \tag{21}$$

Otherwise the process (12) jumps to a new state $\tilde{z}=J(z;i,j,e)$ as described in (15). The distribution of the parameter e is

$$\frac{q(z;i,j,e)}{\int\limits_{S^2} q(z;i,j,e)\,de}. \tag{22}$$

There is a degree of freedom in our method, namely an appropriate choice of the weight transfer function G. This function should always fulfil the condition

$$G(z;i,j,e)\le \min(g_i,g_j)$$

in order to avoid negative weights in (15). We consider the function G in the form

$$G(z;i,j,e)=\frac{\min(g_i,g_j)}{1+\gamma(z;i,j,e)}, \tag{23}$$

where $\gamma(z;i,j,e)\ge 0$ is a parameter of the method which can be chosen arbitrarily, depending on our interest. The parameter γ can vary in different regions of the flow (cell Ω_ℓ), for different collision partners i and j or even as a function of the unit vector e. The jump intensity function q is then defined by the basic relationship (16) as

$$q(z;i,j,e)=(1+\gamma(z;i,j,e))\max(g_i,g_j)\,h_\ell(x_i,x_j)\,B(v_i,v_j,e)\,. \tag{24}$$

According to (18), we need a majorant for the function (24). Note that the function (11) is now just a constant, i.e.

$$h_\ell(x_i,x_j)=\frac{1}{|\Omega_\ell|},$$

because we have assumed that all particles are sorted in cells. Furthermore, we use the majorants

$$\begin{aligned} 1+\gamma(z;i,j,e) &\le 1+C_{\gamma,max}\,, \\ \int\limits_{S^2} B(v_i,v_j,e)\,de &\le C_{B,max}\,, \\ \max(g_i,g_j) &\le g_i+g_j-g_{min}(z)\,, \end{aligned} \tag{25}$$

where

$$g_{min}(z) = \min_{1 \le i \le n} g_i \,, \tag{26}$$

to obtain

$$\hat{q}_{max}(z; i, j) = (1 + C_{\gamma,max})\, C_{B,max} \frac{1}{|\Omega_\ell|}\, (g_i + g_j - g_{min}(z)) \,.$$

Now we are able to compute the waiting time parameter via (17)

$$\hat{\pi}(z) = \frac{1}{2}\,(1 + C_{\gamma,max})\, C_{B,max} \frac{1}{|\Omega_\ell|}\,(n-1)\,(2 g_{sum}(z) - n g_{min}(z))\,, \tag{27}$$

where

$$g_{sum}(z) = \sum_{i=1}^{n} g_i \,, \tag{28}$$

as well as all other parameters of our process. The probability of the parameters i and j is determined via (20)

$$\frac{g_i + g_j - g_{min}(z)}{(n-1)\,(2\, g_{sum}(z) - n\, g_{min}(z))} \,. \tag{29}$$

The parameter i is then to be chosen according to the probability

$$\frac{(n-2)\, g_i + g_{sum}(z) - (n-1)\, g_{min}(z)}{(n-1)\,(2\, g_{sum}(z) - n\, g_{min}(z))} \,.$$

Given i , the parameter j is chosen according to the probability

$$\frac{g_i + g_j - g_{min}(z)}{(n-2)\, g_i + g_{sum}(z) - (n-1)\, g_{min}(z)} \,.$$

Given i and j , the jump is fictitious with probability (21)

$$1 - \frac{\int\limits_{S^2} (1 + \gamma(z; i, j, e))\, B(v_i, v_j, e)\, de}{(1 + C_{\gamma,max})\, C_{B,max}} \frac{\max(g_i, g_j)}{g_i + g_j - g_{min}(z)} \,, \tag{30}$$

otherwise the distribution of the parameter e is (22),

$$\frac{(1 + \gamma(z, i, j, e))\, B(v_i, v_j, e)}{\int\limits_{S^2} (1 + \gamma(z, i, j, e))\, B(v_i, v_j, e)\, de} \,, \tag{31}$$

and the new state is $\tilde{z} = J(z; i, j, e)$ as defined in (15). For the Boltzmann equation (1) with the collision kernel (6) we obtain for the constant $C_{B,max}$

$$\int\limits_{S^2} B(v_i, v_j, e)\, de = \frac{|v_i - v_j|}{\sqrt{2}\, Kn} \le \frac{U_\ell}{\sqrt{2}\, Kn} = C_{B,max} \,, \tag{32}$$

where U_ℓ denotes the maximum relative velocity in the cell Ω_ℓ which has to be estimated in every time step. The corresponding estimate for the Maxwell molecules is trivially

$$\int\limits_{S^2} B(v_i, v_j, e)\, de = 1 = C_{B,max} \,. \tag{33}$$

2.2 Examples of the SWPM

In this subsection we consider three examples for the particular choice for the parameters of the SWPM.

Example 1 *Consider the special case*

$$g_i = g = const \qquad and \qquad \gamma = 0\,.$$

The parameter g_{min} remains constant

$$g_{min} = g\,.$$

The parameter g_{sum} is

$$g_{sum} = g\,n\,.$$

The waiting time parameter $\hat{\pi}(z)$ is for the hard spheres model

$$\hat{\pi}(z) = \frac{1}{2\sqrt{2}\,Kn}\,\frac{U_\ell}{|\Omega_\ell|}\,g\,n\,(n-1)$$

and for the Maxwell molecules

$$\hat{\pi}(z) = \frac{1}{2}\,\frac{1}{|\Omega_\ell|}\,g\,n\,(n-1)\,.$$

The deterministic time counter $\hat{\tau}(z)$ is nothing else than Bird's well-known "no time counter"

$$\hat{\tau}(z) = \frac{2\sqrt{2}\,Kn|\Omega_\ell|}{g\,n\,(n-1)U_\ell}\,.$$

For the Maxwell molecules we obtain

$$\hat{\tau}(z) = \frac{2|\Omega_\ell|}{g\,n\,(n-1)}\,.$$

The index i is uniformly distributed on

$$\{1,\ldots,n\}\,.$$

Given i, the index j is uniformly distributed on

$$\{1,\ldots,n\} \setminus \{i\}\,.$$

Given i and j, the weight transfer function G is

$$G = g\,.$$

For the hard spheres model the jump is fictitious with probability

$$1 - \frac{|v_i - v_j|}{U_\ell}\,.$$

There are no fictitious jumps for the Maxwell molecules.

The parameter e is uniformly distributed on the unit sphere S^2.

There is no increase in the number of particles in the system. The particles for $k=i$ and $k=j$ in (15) have zero weights and should therefore be removed from the system. Here we would like to point out that our SWPM is a generalisation of the Bird's DSMC method.

Example 2 *Consider the second special case*

$$g_i - \textit{arbitrary} \qquad \textit{and} \qquad \gamma = 0\,.$$

The parameter g_{min} should be updated after every collision

$$g_{min} = \min_{1\le i\le n} g_i\,.$$

The parameter g_{sum} is

$$g_{sum} = \sum_{i=1}^{n} g_i,\,.$$

The waiting time parameter $\hat{\pi}(z)$ is for the hard spheres model

$$\hat{\pi}(z) = \frac{1}{2\sqrt{2}\,Kn}\,\frac{U_\ell}{|\Omega_\ell|}\,(n-1)\,(2\,g_{sum}(z) - n\,g_{min}(z))\,.$$

and for the Maxwell molecules

$$\hat{\pi}(z) = \frac{1}{2}\,\frac{1}{|\Omega_\ell|}\,(n-1)\,(2g_{sum}(z) - ng_{min}(z))\,.$$

The deterministic time counter is always

$$\hat{\tau}(z) = (\hat{\pi}(z))^{-1}\,.$$

The index i is to be chosen according to the probability

$$\frac{(n-2)\,g_i + g_{sum}(z) - (n-1)\,g_{min}(z)}{(n-1)\,(2\,g_{sum}(z) - n\,g_{min}(z))}\,.$$

Given i, the index j is chosen according to the probability

$$\frac{g_i + g_j - g_{min}(z)}{(n-2)\,g_i + g_{sum}(z) - (n-1)\,g_{min}(z)}\,.$$

Given i and j, the weight transfer function G is

$$G = \min(g_i, g_j)\,.$$

The jump is fictitious with probability

$$1 - \frac{|v_i - v_j|}{U_\ell}\,\frac{\max(g_i, g_j)}{g_i + g_j - g_{\min}(z)}$$

for the hard spheres and

$$1 - \frac{\max(g_i, g_j)}{g_i + g_j - g_{\min}(z)}$$

for the Maxwell molecules.

The parameter e is uniformly distributed on the unit sphere S^2.

The number of particles increases by one in each collision with unequal weights, according to (15). If all initial particles and all inflow particles have the same weight then this case is identical to the previous one.

Example 3 *Consider the third special case*

$$g_i - \textit{arbitrary} \qquad \textit{and} \qquad \gamma = const > 0\,.$$

In this case the waiting time parameter $\hat{\pi}(z)$ *for the hard spheres model is*

$$\hat{\pi}(z) = \frac{1+\gamma}{2\sqrt{2}\,Kn}\,\frac{U_\ell}{|\Omega_\ell|}\,(n-1)\,(2\,g_{sum}(z) - n\,g_{min}(z))\,.$$

and for the Maxwell molecules

$$\hat{\pi}(z) = \frac{1+\gamma}{2}\,\frac{1}{|\Omega_\ell|}\,(n-1)\,(2g_{sum}(z) - ng_{min}(z))$$

leading to the corresponding change for the deterministic time counter

$$\hat{\tau}(z) = (\hat{\pi}(z))^{-1}\,.$$

All other parameters of the process remain the same.

In this case the number of particles increases by two in each collision. This procedure can be used efficiently to reduce stochastic fluctuations arising in computation of the macroscopic quantities in regions with low particle density, as we showed in [RW96a].

But the new small particles move and will probably reach the region where the particle density is normal. There it is necessary to use the second special case (Example 2) for the collisions, which means that the number of particles will increase further without any advantage being gained. The best situation is, of course, if the particles disappear through the "outflow boundary" of the computational domain at a rate corresponding to the "production rate" there. In such a situation we will still be dealing with an asymptotically constant number of particles, but with more small particles in the low density regions (this is our improvement) which are producing more small and probably useless particles on the way to the "outflow boundary" (this is the price). In all other situations reduction of the number of particles is necessary.

2.3 Reduction of Particles

In [RSW98] we give a systematic study of the theoretical and numerical aspects of reducing the number of particles including the theoretical estimates for the error of the reduction in the bounded Lipschitz metric as well as in the Sobolev space $\mathbb{H}^{-2}$. In [MW02] the authors introduce a purely stochastic reduction procedure and prove the convergence of the SWPM with such reductions. In the present paper we give a short summary of these results. First of all we introduce an additional parameter $n_{max} > 0$ which determines some bound for the number of particles in the system. Then we change the transition measure (14) to

$$Q(z; d\tilde{z}) = \begin{cases} Q_{coll}(z; d\tilde{z}), & \text{if} \quad n < n_{max} \\ Q_{red}(z; d\tilde{z}), & \text{if} \quad n \geq n_{max} \end{cases} . \tag{34}$$

The transition measure, corresponding to collisions, remains unchanged (cf. (14))

$$Q_{coll}(z; d\tilde{z}) = \frac{1}{2} \sum_{1 \leq i \neq j \leq n} \int_{S^2} \delta_{J(z;i,j,e)}\, q(z; i, j, e)\, de\,,$$

while the transition measure, corresponding to reductions, has the following form

$$Q_{red}(z; d\tilde{z}) = \lambda_{red} P_{red}(z; d\tilde{z})\,, \tag{35}$$

where $\lambda_{red} > 0$ is some waiting time parameter and P_{red} is the reduction measure. The procedure of reduction contains two steps. The first step is the dividing of the whole particle system (10) in a set of clusters in velocity space, i.e. groups of particles having almost the same velocities. Then the reduction of particles takes place clusterwise, i.e. each cluster will be replaced by few (one or two as a rule) particles. The construction of the clusters we use completely deterministic recursive procedure which can be explained as follows. Let

$$z = \Big(g_j, x_j, v_j\Big)_{j=1}^{n_c} \tag{36}$$

be a cluster of particles which is identical at the beginning of the recursion with a given system (10). Then we compute the mass, the mean velocity and the covariance matrix of this cluster

$$\varrho(z) = \sum_{i=1}^{n_c} g_j \in \mathbb{R}_+\,, \tag{37}$$

$$V(z) = \frac{1}{\varrho(z)} \sum_{i=1}^{n_c} g_j\, v_j \in \mathbb{R}^3, \tag{38}$$

$$M(z) = \frac{1}{\varrho(z)} \sum_{i=1}^{n_c} g_j\, (v_j - V)(v_j - V)^\top \in \mathbb{R}^3 \times \mathbb{R}^3. \tag{39}$$

Then we divide the cluster (36) in two sons using the criterion

$$(v_i - V, e_{max}) \ \begin{matrix} \leq \\ > \end{matrix} \ 0\,. \tag{40}$$

Here e_{max} denotes the eigenvector of M corresponding to its largest eigenvalue. Then we continue dividing the sons of the initial cluster in the same manner. This procedure stops if an admissible cluster has less particles as will be required by the reduction or if the desired number of clusters is reached and all of them are admissible. There are several possibilities to reduce the number of particles in an admissible cluster

$$z = \left(g_j, x_j, v_j\right)_{j=1}^{n_c}$$

to one or two. Here we give two examples.

Example 4 *The cluster is admissible for the reduction if its "mass" $\varrho(z)$ is less then some global upper bound for the particle weight $g_{\max}$. Choose the index i corresponding to discrete probabilities $g_i/\varrho(z)$ and replace the cluster by one particle*

$$\tilde{z} = J_{red,1}(z;i) = \left(\varrho(z), x_i, v_i\right).$$

In this case we have

$$p_{red,1}(z;d\tilde{z}) = \frac{1}{\varrho(z)} \sum_{i=1}^{n_c} \delta_{J_{red,1}(z;i)}(d\tilde{z}).$$

This reduction conserves the mass of the cluster while the momentum and the energy are not conserved. However, the expectation of all linear functionals of the form

$$\int_{\mathcal{Z}} \Phi(\tilde{z})\, p_{red,1}(z;d\tilde{z}) \tag{41}$$

with

$$\Phi(z) = \sum_{i=1}^{n_c} g_i\, \varphi(x_i, v_i) \tag{42}$$

for an arbitrary test function φ does not change

$$\int_{\mathcal{Z}} \Phi(\tilde{z}) p_{red,1}(z;d\tilde{z}) = \tag{43}$$

$$\sum_{i=1}^{n_c} \frac{g_i}{\varrho(z)}\, \Phi\left(J_{red,1}(z;i)\right) = \sum_{i=1}^{n_c} \frac{g_i}{\varrho(z)}\, \varrho(z)\, \varphi(x_i, v_i) = \Phi(z). \tag{44}$$

Thus this reduction procedure conserves the mass exactly and in average all other usual moments.

Example 5 *The cluster is admissible for the reduction if its "mass" $\varrho(z)$ is less then $2\, g_{\max}$. Choose the unit vector $e \in S^2$ corresponding to the uniform measure on S^2 and replace the cluster by two particles*

$$\left(J_{red,2}(z;i,j,e)\right)_1 = \left(\frac{\varrho(z)}{2}, x_i, V + \sqrt{\mathrm{tr} M}\; e\right),$$
$$\left(J_{red,2}(z;i,j,e)\right)_2 = \left(\frac{\varrho(z)}{2}, x_j, V - \sqrt{\mathrm{tr} M}\; e\right).$$

In this case we have

$$\tilde{z} = \left((J_{red,2}(z;i,j,e))_1\,, (J_{red,2}(z;i,j,e))_2 \right)$$

and

$$p_{\mathrm{red},2}(z;d\tilde{z}) = \frac{1}{\varrho^2(z)} \sum_{i,j=1}^{n_c} g_i\, g_j \int\limits_{S^2} \delta_{J_{\mathrm{red},2}(z;i,j,e)}(d\tilde{z})\, de\,.$$

Note that two particles are produced. Each of them is given half of the weight of the original cluster. Their velocities are determined by the conservation of momentum and energy up to a random vector $e \in S^2$. Thus this reduction procedure is full conservative. However, the expectation of the general functionals (42) will differ from the exact value.

We refer to [Sch93] and [RSW98] for more examples of reductions.

The global reduction measure (35) is then defined as product of the cluster reduction measures which are assumed to be independent of each other.

2.4 Theoretical Foundation and Convergence

We consider the bounded Lipschitz metric

$$\varrho_L(m_1, m_2) = \sup_{||\varphi||_L \le 1} \left| \int\limits_{\Omega\times\mathbb{R}^3} \varphi(x,v)\, m_1(dx,dv) - \int\limits_{\Omega\times\mathbb{R}^3} \varphi(x,v)\, m_2(dx,dv) \right|$$

on the space $\mathcal{M}(\Omega \times \mathbb{R}^3)$ of finite Borel measures on $\Omega \times \mathbb{R}^3$. Here the notations

$$||\varphi||_L = \max\left\{ ||\varphi||_\infty\,, \sup_{(x,v)\neq(y,w)\in\Omega\times\mathbb{R}^3} \frac{|\varphi(x,v) - \varphi(y,w)|}{|x-y| + |v-w|} \right\} \tag{45}$$

and

$$||\varphi||_\infty = \sup_{(x,v)\in\Omega\times\mathbb{R}^3} |\varphi(x,v)| \tag{46}$$

are used.

Let $n \in \mathbb{N}$ be some parameter connected to the number of particles in the system which will be now denoted by $n_s^{(n)}$. Thus all parameters of the SWPM are now assumed to be functions of n.

The following assumptions have to be made in order to formulate the convergence result of the SWPM with reductions.

1. The physical domain Ω is assumed to be compact.

2. The global particle weight bound satisfies
$$\lim_{n\to\infty} g_{\max}^{(n)} \;=\; 0\,. \tag{47}$$

3. The particle number bound indicating reduction (cf. (34)) satisfies
$$\lim_{n\to\infty} n_{\max}^{(n)} \;=\; \infty\,. \tag{48}$$

4. The parameter of the waiting time before reduction (cf. (35)) satisfies
$$\lim_{n\to\infty} \lambda_{\mathrm{red}}^{(n)} \;=\; \infty\,. \tag{49}$$

5. The reduction effect is sufficiently strong, i.e.
$$P_{\mathrm{red}}^{(n)}(z;\mathcal{Z}^{(n)}(\delta)) = 1\,, \qquad \forall\, z \in \mathcal{Z}^{(n)} \setminus \mathcal{Z}^{(n)}(0)\,, \tag{50}$$
for some $\delta \in (0,1)$, where the notation
$$\mathcal{Z}^{(n)}(\delta) = \Big\{ z \in \mathcal{Z}^{(n)} \,:\, n_s \le (1-\delta)\, n_{\max}^{(n)} \Big\}$$
is used. Note that
$$\mathcal{Z}^{(n)} \setminus \mathcal{Z}^{(n)}(0) = \Big\{ z \in \mathcal{Z}^{(n)} \,:\, n_s > n_{\max}^{(n)} \Big\}$$
is the set of all possible starting points of a reduction jump.

6. The reduction is sufficiently precise, i.e.
$$\lim_{n\to\infty} \sup_{\varphi\in D_r} \sup_{z\in\mathcal{Z}^{(n)}\setminus\mathcal{Z}^{(n)}(0)} \sum_{i\in I_r^{(n)}(z)} \left| \Phi(z_i) - \int_{\mathcal{Z}^{(n)}} \Phi(\tilde{z}_i)\, P_{\mathrm{red},i}^{(n)}(z_i;d\tilde{z}_i) \right| = 0\,, \tag{51}$$
for any Φ of the form (42) and for any $r>0$. The set D_r in (51) is defined as follows
$$D_r = \Big\{ \varphi_r \,:\, \|\varphi\| \le 1 \Big\} \tag{52}$$
where
$$\varphi_r(x,v) = \begin{cases} \varphi(x,v) & , \quad |v| \le r, \\ (r+1-|v|)\varphi(x,v) & , \quad r < |v| \le r+1, \\ 0 & , \quad |v| > r+1. \end{cases} \tag{53}$$
The particle system z is decomposed in clusters. The index set $I_r^{(n)}(z)$ contains the indices of only such clusters which contain particles having velocities within the ball $B_r(0)$
$$I_r^{(n)}(z) = \Big\{ i \,:\, z_i \cap \{(x,v,g) \,:\, |v| < r\} \neq \emptyset \Big\} \tag{54}$$
Note that this technically complicated assumption is trivially fulfilled for the stochastic reduction from Example 4 because of the property (43).

7. The reduction conserves the mass, i.e.
$$\varrho(\tilde{z}) = \varrho(z)\,. \tag{55}$$
8. The energy of the system after every reduction fulfils
$$\int\limits_{\mathcal{Z}^{(n)}} \operatorname{tr} M(\tilde{z})\, p_{\mathrm{red}}^{(n)}(z; d\tilde{z}) \le c \operatorname{tr} M(z)$$
for some constant $c > 0$.

Now we are able to formulate the convergence theorem.

Theorem 6 *Let F be a function of time $t \ge 0$ with values in $\mathcal{M}(\Omega \times \mathbb{R}^3)$ satisfying the equation*
$$\int\limits_{\Omega\times\mathbb{R}^3} \varphi(x,v)\, F(t,dx,dv) = \int\limits_{\Omega\times\mathbb{R}^3} \varphi(x,v)\, F_0(dx,dv) +$$
$$\frac{1}{2}\int\limits_0^t \int\limits_{\Omega\times\mathbb{R}^3}\int\limits_{\Omega\times\mathbb{R}^3}\int\limits_{S^2} \Big(\varphi(x,v') + \varphi(y,w') - \varphi(x,v) - \varphi(y,w)\Big) \times$$
$$h(x,y)\, B(v,w,e)\, de\, F(s,dx,dv)\, F(s,dy,dw)\, ds\,,$$
for all test functions φ on $\Omega \times \mathbb{R}^3$ such that $\|\varphi\|_L < \infty$.

Assume that the solution satisfies
$$\sup_{t\in[0,S]} F(t, \Omega \times \mathbb{R}^3) \le c(S)\, F_0(\Omega \times \mathbb{R}^3)$$
and
$$\sup_{t\in[0,S]} \int\limits_{\Omega\times\mathbb{R}^3} |v|^2\, F(t,dx,dv) \le c(S) \int\limits_{\Omega\times\mathbb{R}^3} |v|^2\, F_0(dx,dv)\,,$$
for arbitrary $S \ge 0$ and some constants $c(S) > 0$.

Assume that the process parameters satisfy all assumptions formulated above.

Let
$$\mu^{(n)}(t,dx,dv) = \sum_{i=1}^{n_s^{(n)}(t)} g_i^{(n)}(t)\, \delta_{x_i^{(n)}(t)}(dx)\, \delta_{v_i^{(n)}(t)}(dv)\,, \quad t \ge 0$$
denote the sequence of empirical measures of the processes (12). If
$$\lim_{n\to\infty} \mathbb{E}\, \varrho_L(\mu^{(n)}(0), F_0) = 0$$
and
$$\limsup_{n\to\infty} \mathbb{E} \int\limits_{\Omega\times\mathbb{R}^3} |v|^2\, \mu^{(n)}(0,dx,dv) < \infty$$
then
$$\lim_{n\to\infty} \mathbb{E} \sup_{t\in[0,S]} \varrho_L(\mu^{(n)}(t), F(t)) = 0\,, \quad \forall\, S > 0\,.$$

3 Numerical examples and tests

3.1 Statistical notions

First we introduce some definitions and notations that are helpful for the understanding of stochastic numerical procedures. Functionals of the form

$$F(t) = \int_{\mathbb{R}^3} \varphi(v)\, f(t,v)\, dv\,. \tag{56}$$

are approximated by the random variable

$$\xi^{(n)}(t) = \frac{1}{n} \sum_{i=1}^{n} \varphi(v_i(t))\,, \tag{57}$$

here $(v_1(t), \ldots, v_n(t))$ are the velocities of the particle system. In order to estimate and to reduce the random fluctuations of the estimator (57), a number N of independent ensembles of particles is generated. The corresponding values of the random variable are denoted by

$$\xi_1^{(n)}(t), \ldots, \xi_N^{(n)}(t)\,.$$

The **empirical mean value** of the random variable (57)

$$\eta_1^{(n,N)}(t) = \frac{1}{N} \sum_{j=1}^{N} \xi_j^{(n)}(t) \tag{58}$$

is then used as an approximation to the functional (56). The error of this approximation is

$$e^{(n,N)}(t) = |\eta_1^{(n,N)}(t) - F(t)|$$

and consists of the following two components.

The **systematic error** is the difference between the mathematical expectation of the random variable (57) and the exact value of the functional, i.e.

$$e_{sys}^{(n)}(t) = E\xi^{(n)}(t) - F(t)\,.$$

The **statistical error** is the difference between the empirical mean value and the expected value of the random variable, i.e.

$$e_{stat}^{(n,N)}(t) = \eta_1^{(n,N)}(t) - E\xi^{(n)}(t)\,.$$

A **confidence interval** for the expectation of the random variable $\xi^{(n)}(t)$ is obtained as

$$I_p = \left[\eta_1^{(n,N)}(t) - \lambda_p \sqrt{\frac{\operatorname{Var} \xi^{(n)}(t)}{N}}\,,\ \eta_1^{(n,N)}(t) + \lambda_p \sqrt{\frac{\operatorname{Var} \xi^{(n)}(t)}{N}} \right], \tag{59}$$

where

$$\operatorname{Var}\xi^{(n)}(t) := E\left[\xi^{(n)}(t) - E\xi^{(n)}(t)\right]^2 = E\left[\xi^{(n)}(t)\right]^2 - \left[E\xi^{(n)}(t)\right]^2 \tag{60}$$

is the **variance** of the random variable (57), and $p \in (0,1)$ is the **confidence level**. This means that

$$\operatorname{Prob}\left\{E\xi^{(n)}(t) \notin I_p\right\} = \operatorname{Prob}\left\{|e_{stat}^{(n,N)}(t)| \geq \lambda_p \sqrt{\frac{\operatorname{Var}\xi^{(n)}(t)}{N}}\right\} \sim p\,.$$

Thus, the value

$$c^{(n,N)}(t) = \lambda_p \sqrt{\frac{\operatorname{Var}\xi^{(n)}(t)}{N}}$$

is a probabilistic upper bound for the statistical error.

In the calculations we use a confidence level of $p = 0.999$ and $\lambda_p = 3.2$. The variance is approximated by the corresponding empirical value (cf. (60)), i.e.

$$\operatorname{Var}\xi^{(n)}(t) \sim \eta_2^{(n,N)}(t) - \left(\eta_1^{(n,N)}(t)\right)^2,$$

where

$$\eta_2^{(n,N)}(t) = \frac{1}{N}\sum_{j=1}^{N}\left(\xi_j^{(n)}(t)\right)^2$$

is the **empirical second moment** of the random variable (57).

3.2 Spatially homogeneous Boltzmann Equation

In this subsection we consider two examples for spatially homogeneous Boltzmann equation

$$\frac{\partial}{\partial t} f = Q(f,f) \tag{61}$$

for the distribution function $f : \mathbb{R}_+ \times \mathbb{R}^3 \to \mathbb{R}_+$ in the case of Maxwell molecules, i.e. for the constant collision kernel (7).

We consider first the most simple example if the initial distribution is a normalised Maxwell distribution

$$f_0(v) = \frac{1}{(2\,\pi)^{3/2}} \exp\left(-\frac{|v|^2}{2}\right), \quad v \in \mathbb{R}^3. \tag{62}$$

Since this function exactly solves the Boltzmann equation (61), i.e.

$$f(t,v) = f_0(v)\,, \quad \forall\, t \geq 0$$

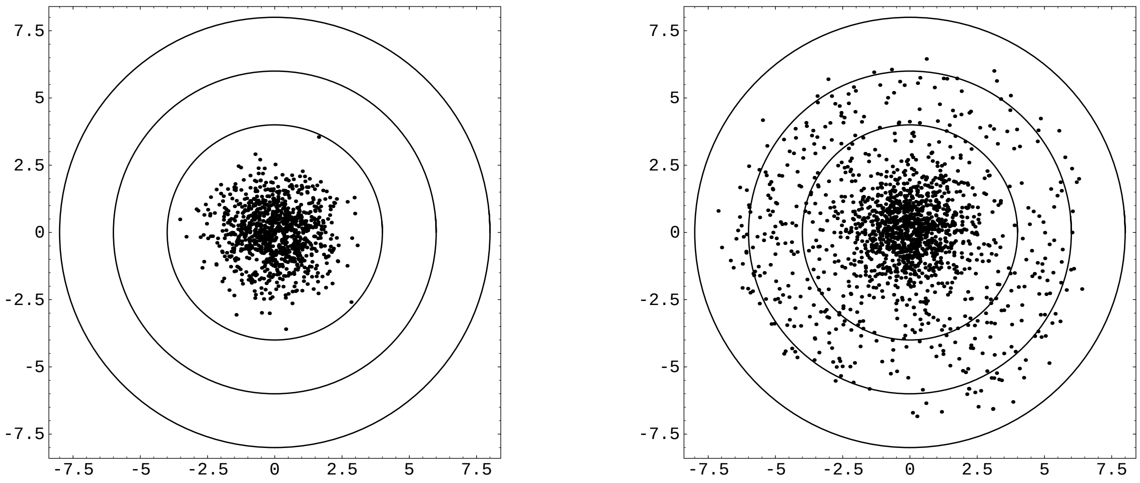

Figure 1: Initial and "final" distributions of SWPM particles

all its moments and functionals remain constant in time.

Using SWPM we are able to resolve the velocity space much better than using particles with constant weights. For example, we are able to compute very small functionals using relatively low number of particles. As a model of such small functionals, or "rare events", we will consider "tail" functionals

$$\mathrm{Tail}(t,R) = \int\limits_{|v|\geq R} f(t,v)\,dv\,, \tag{63}$$

describing the portion of particles outside the ball of radius R centred in the origin at time t. If f is a Maxwell distribution (62) then its tail functional is constant in time and can be computed analytically

$$\mathrm{Tail}(R) = 1 - \mathrm{erf}\Big(\frac{R}{\sqrt{2}}\Big) + \frac{2}{\sqrt{\pi}}\,R\,\exp\Big(-\frac{R^2}{2}\Big)\,. \tag{64}$$

In the next figures we illustrate how the particles occupy a bigger and bigger part of the velocity space during the time. We use

$$n(0) = 1\,024\,,\ n_{max} = 4\,096\,,\ g_{max} = 2/n(0)\,,$$

and generate one ensemble of particles by the SWPM algorithm with stochastic reduction (see Example 4) on the time interval $[0,16]$. The left plot of Fig. 1 shows the projections of three-dimensional velocities of 1024 particles into the plane $v_1 \times v_2$ while the right plot shows the "final" picture after 64 reductions for $n(t) = 1234$ particles. It is clear to see that having almost the same number of particles the new system is rather different from the initial picture. Now only half of all particles is responsible for the resolution of the main stream within the ball $|v| \leq 4$ while the second half of particles is more or less uniformly distributed within much bigger ball $|v| \leq 8$. Thus the new system of particles can be successfully used for the

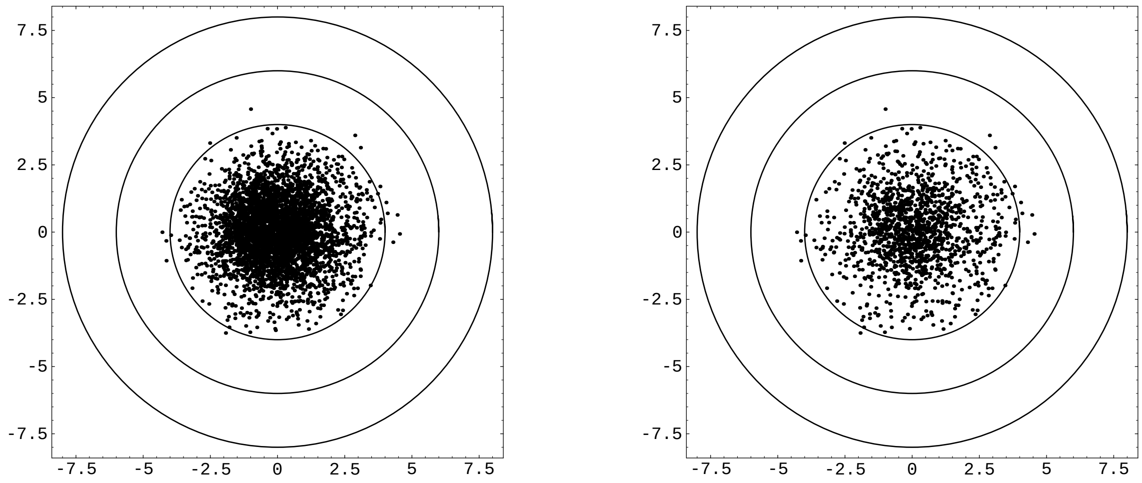

Figure 2: 4th reduction of particles

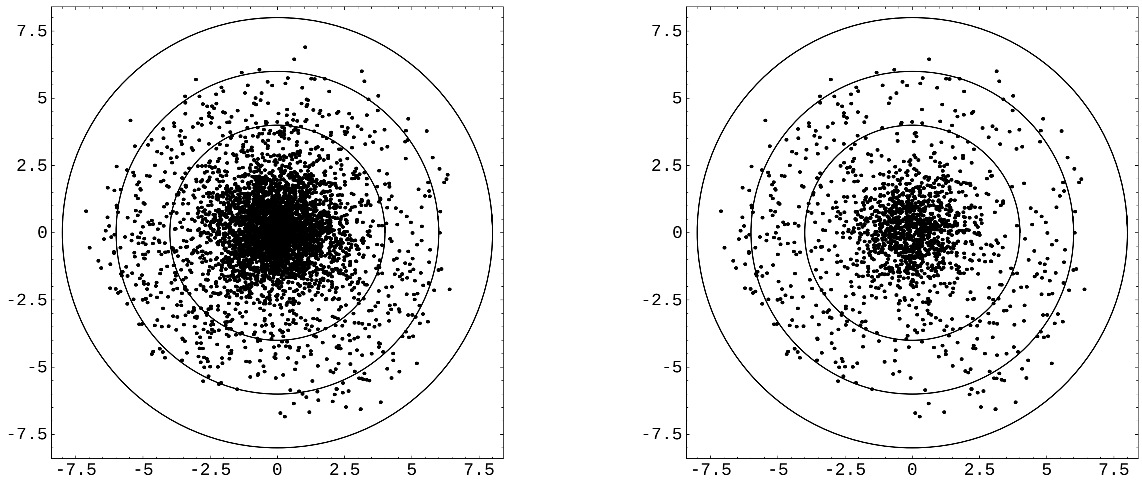

Figure 3: 64th reduction of particles

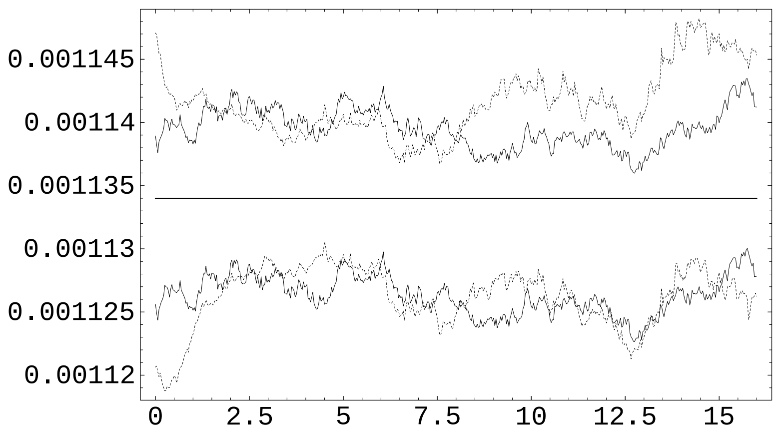

Figure 4: Tail functional for $R = 4$

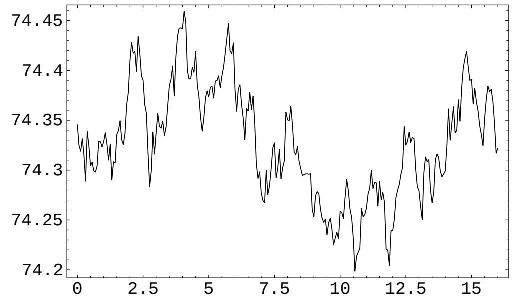

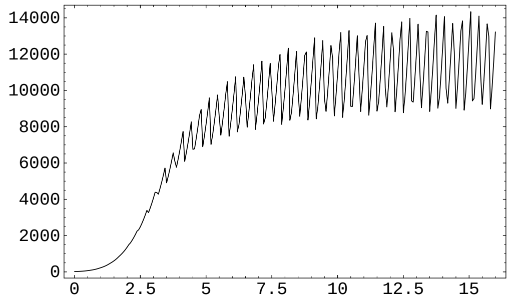

Figure 5: Number of particles in the tail for $R = 4$

estimation of very rare events, e.g. for the tail functionals (64). The 4th and the 64th reductions of particles are illustrated in Figs. 2-3. It is important that the "useful" but small particles living in the plotted tails will be not destroyed during the reduction. Thus the system of particles uniformly occupies bigger and bigger part of the velocity space during the collisions.

Now we are going to illustrate the numerical computation of the tails

$$\mathrm{Tail}(4) = 0.113398\ldots \cdot 10^{-3}\,,\ \mathrm{Tail}(6) = 0.748837\ldots \cdot 10^{-7} \tag{65}$$

using both DSMC and SWPM methods. We solve the Boltzmann equation with DSMC using $n = 65\,536$ particles and generating $N = 4\,096$ independent ensembles. Using SWPM, we start with $n(0) = 16\,384$ particles and reduce the number of particles corresponding to Example 4 at each time point t with $n(t) = 65\,536$. The computational time for $N = 4\,096$ independent ensembles is then similar to the corresponding time of DSMC. Figs. 4 and 6 show the analytical values for the tails (65) (thick solid lines), the confidence intervals obtained using DSMC (thin solid lines) and the confidence intervals obtained using SWPM (thin dotted lines).

Figs. 5 and 7 show the average number of particles forming the tails. Here the left plots corresponds to DSMC and the right plots to SWPM. We can see that

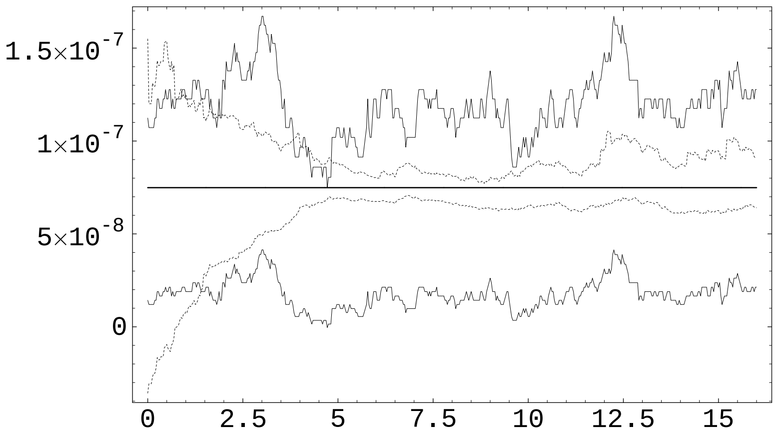

Figure 6: Tail functional for $R = 6$

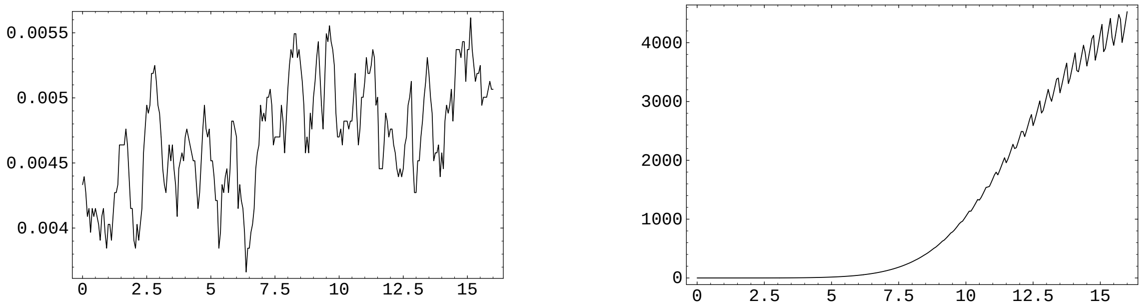

Figure 7: Number of particles in the tail for $R = 6$

at the begin of the simulation the width of the confidence intervals is better for DSMC due to the higher number of particles. The number of particles forming the tail remains almost constant for DSMC. The corresponding number increases using SWPM leading to smaller confidence intervals. The width of the DSMC confidence intervals is four-five times larger for $R = 6$. Thus SWPM can be considered 16-25 times "faster" computing this tail with similar accuracy.

In the next example we study the famous exact solution found by Bobylev [Bob75] and Krook and Wu [KW77]

$$f(t,v) = \frac{1}{(2\,\pi)^{3/2}}\,(\beta(t)+1)^{3/2}\,\left(1+\beta(t)\Big(\frac{\beta(t)+1}{2}|v|^2-\frac{3}{2}\Big)\right)\,e^{-\frac{\beta(t)+1}{2}|v|^2}\,, \tag{66}$$

where

$$\beta(t) = \frac{2\,e^{-t/6}}{5-2\,e^{-t/6}}\,.$$

Note that the tail functional (63) can be given for the solution (66) in the closed

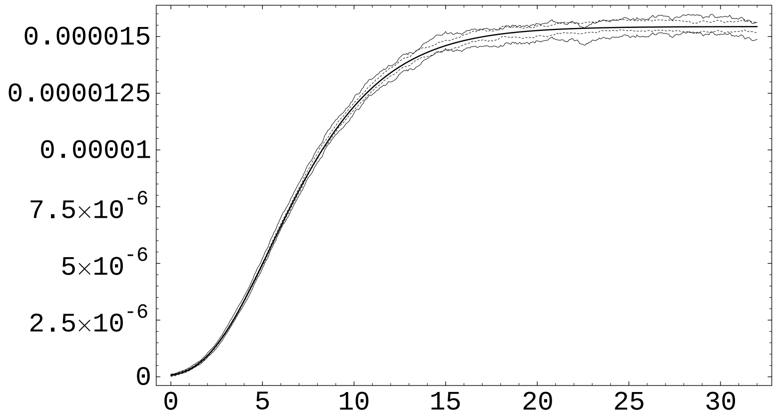

Figure 8: Tail functional (67) for $R = 5$

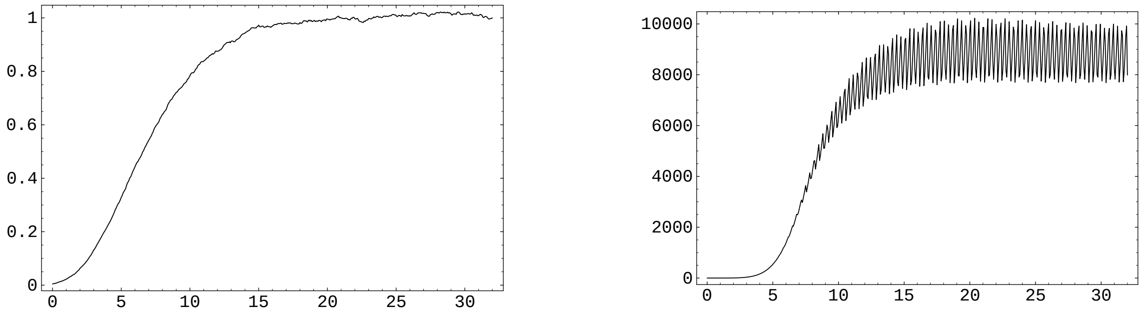

Figure 9: Number of particles in the tail for $R = 5$

form

$$\mathrm{Tail}(t,R) = 1 - \mathrm{erf}\Big(\sqrt{\frac{\beta(t)+1}{2}}\,R\Big) + \\ \frac{2}{\sqrt{\pi}}\sqrt{\frac{\beta(t)+1}{2}}R\Big(1+\beta(t)R^2\frac{\beta(t)+1}{2}\Big)\exp\Big(-\frac{\beta(t)+1}{2}\,R^2\Big). \tag{67}$$

We study the time relaxation of the tail functional (67) on the time interval $[0,32]$ using both DSMC and SWPM algorithms. The number of particles for DSMC is $n = 65\,536$. SWPM (with the stochastic reduction algorithm from Example 4) is started using $n = 16\,384$ particles. We reduce the number of particles at each time point t with $n(t) = 65\,536$. The number of independent ensembles is $N = 16\,384$. The computational time is similar for both methods.

In the figures confidence intervals obtained using DSMC are shown by thin solid lines, while confidence intervals obtained using SWPM are shown by thin dotted lines. The analytical curves of the tails (67) are displayed by thick solid lines. In the figures showing the average numbers of particles forming the tails, the left plots corresponds to DSMC and the right plots to SWPM. The resolution of the tail with $R = 5$ is already better for SWPM as shown in Fig. 8. In other words, SWPM is

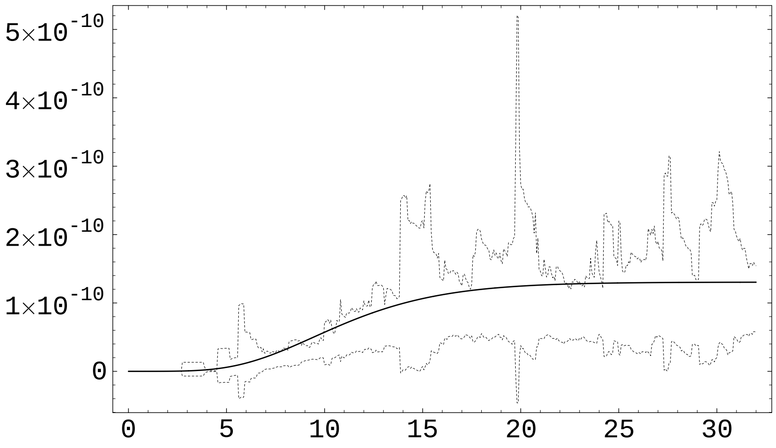

Figure 10: Tail functional (67) for $R = 7$

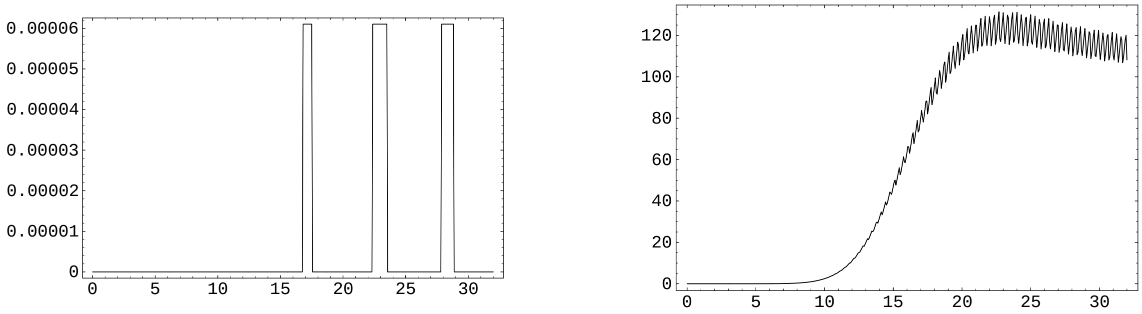

Figure 11: Number of particles in the tail for $R = 7$

two-three times "faster" computing this tail with similar accuracy. Fig. 9 displays the corresponding numbers of particles.

Figs. 10 and 11 show the results obtained using SWPM for the tail with $R = 7$. There are no stable DSMC results for this very small tail, while SWPM reproduces the analytical curve on the whole time interval.

3.3 Spatially 2-dimensional Boltzmann Equation

In this chapter we shall consider some steady state problems for the spatially 2−dimensional Boltzmann equation

$$(v, \mathrm{grad}_x f) = Q(f, f)\,, \tag{68}$$

i.e. the problems in which the distribution function

$$f \;:\; \Omega \times \mathbb{R}^3 \to \mathbb{R}_+\,,\ \Omega \subset \mathbb{R}^3$$

depends only on two Cartesian coordinates x_1 and x_2 as well as on three-dimensional velocity variable v. Now we consider the hard spheres model (6)

$$B(v,w,e) = \frac{1}{4\sqrt{2}\,\pi\,Kn}\,|v-w|\,.$$

There are no analytical solution of the Boltzmann equation in spatially non-homogeneous case. Thus we consider first the free flow equation (i.e. the case $Kn \to \infty$)

$$(v, \mathrm{grad}_x f) = 0 \tag{69}$$

in order to obtain some analytical information. Let Ω be a half space

$$\Omega = \left\{ x \in \mathbb{R}^3 \,:\, x_1 > 0 \right\}$$

The equations (68), (69) are subjected to the following boundary condition

$$f(x,v) = f_{in}(x,v)\,,\;\; x \in \Gamma\,, \tag{70}$$

where

$$\Gamma = \{x = (x_1, x_2, x_3) \in \mathbb{R}^3,\;\; x_1 = 0\} \tag{71}$$

and the inflow function vanishes outside the strip

$$\Gamma_{in} = \left\{ x \in \mathbb{R}^3,\;\; x_1 = 0\,,\;\; -b \le x_2 \le b\,, x_3 \in \mathbb{R} \right\} \tag{72}$$

and is defined for $(v, n_x) = v_1 > 0$ on Γ as follows

$$f_{in}(x,v) = \begin{cases} f_M(v) & , \quad x \in \Gamma_{in} \\ 0 & , \quad \text{otherwise} \end{cases}\,. \tag{73}$$

The Maxwell distribution function f_M having constant physical parameters ϱ_{in}, $V_{in} = (V,0,0)^T$ and T_{in} is

$$f_M(v) = \frac{\varrho_{in}}{(2\pi\,T_{in})^{3/2}} \exp\left(-\frac{|v-V_{in}|^2}{2\,T_{in}}\right). \tag{74}$$

Furthermore we assume that the distribution function f vanishes at infinity

$$\lim_{|x|\to\infty} f(x,v) = 0$$

uniformly with respect to v. The solution of the boundary value problem (69),(70) is given by the formula

$$f(x,v) = f_{in}(x + t\,v, v),\;\; t \in \mathbb{R}, \tag{75}$$

where

$$t = t(x,v) = -\frac{x_1}{v_1}$$

is chosen such that

$$x + t\,v \in \Gamma.$$

The spatial density for this example has been analytically obtained in [RW01] in the following form

$$\varrho(x) = \tag{76}$$
$$\frac{\varrho_{in}}{2\sqrt{\pi}} \int_0^\infty \exp\Big(-(z_1-\xi)^2\Big)\left(\operatorname{erf}\left(\frac{x_2+b}{x_1}\,z_1\right) - \operatorname{erf}\left(\frac{x_2-b}{x_1}\,z_1\right)\right) dz_1\,.$$

Note that the density is a symmetric function with respect to the plane $x_2 = 0$. We calculate the density along the vertical straight line

$$x = \begin{pmatrix} 1 \\ 0.005 \\ 0 \end{pmatrix} + \lambda \begin{pmatrix} 0 \\ 1 \\ 0 \end{pmatrix}, \qquad 0 \le \lambda \le 0.99\,. \tag{77}$$

We assume

$$b = 0.4\,,\;\; \varrho_{in} = 1\,,\;\; T_{in} = 10$$

and define the inflow velocity in the form

$$V_{in} = Mach\,\sqrt{\frac{5}{3}\,T_{in}}\begin{pmatrix} 1 \\ 0 \\ 0 \end{pmatrix}. \tag{78}$$

The inflow Mach number $Mach$ will vary in the subsequent numerical experiments. First we choose the inflow Mach number in (78) equal to 5.0 and solve the the Boltzmann equation within the square $\Omega = (0.0, 2.0) \times (-1.0, 1.0)$. Thus we restrict the unbounded half-space domain to this square. The square Ω will be uniformly discretised in $N_c = 200 \times 200$ spatial cells. Since in the collisionless case there is no mechanism to produce more particles within the computational domain we start the better resolution of the velocity space directly on the inflow boundary (72). To this end we generate only a portion $0 < c_{in} < 1$ of particles corresponding to the boundary condition (73) while the remaining part $1 - c_{in}$ of particles will be generated corresponding to the Maxwell distribution of the form (62) but with higher temperature

$$f_M^\tau(v) = \frac{\varrho_{in}}{(2\pi\,\tau\,T_{in})^{3/2}} \exp\left(-\frac{|v - V_{in}|^2}{2\,\tau\,T_{in}}\right), \tag{79}$$

where $\tau > 1$ is an additional parameter. Thus we are able to place artificially more particles in the tail region of the prescribed distribution function. The parameter $c_{in} \in [0, 1]$ controls the proportion of such particles. The particles generated will have different weights corresponding to the following formula

$$g_i = g\,\frac{1}{c_{in} + (1 - c_{in}) f_M^\tau(v_i)/f_M(v_i)}\,. \tag{80}$$

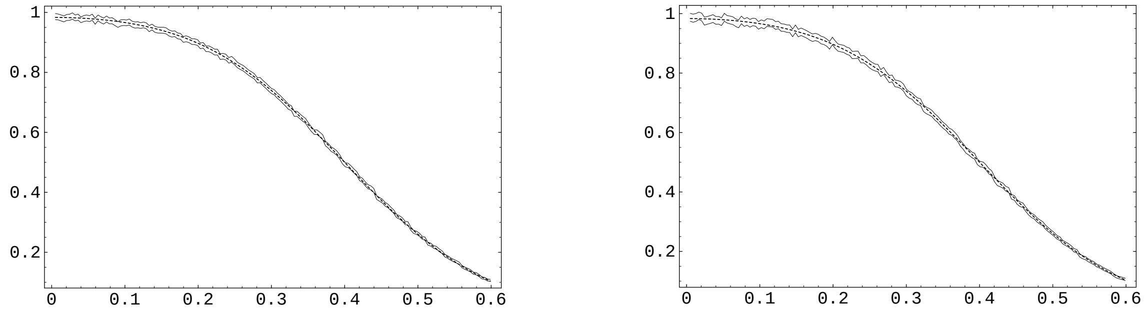

Figure 12: “High” density region, $Mach = 5.0$

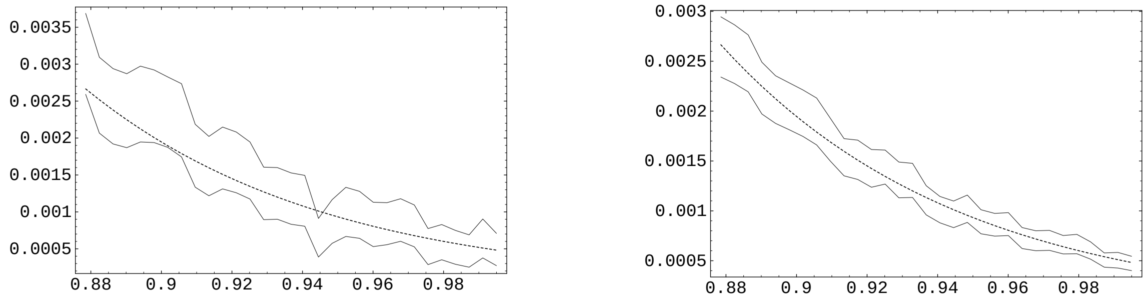

Figure 13: “Low” density region, $Mach = 5.0$

We will use $c_{in} = 1/2$ and $\tau = 8$ in all subsequent examples.

Fig. 12 shows the analytic expression for the density (76) (thick dashed line) and the confidence bands (thin lines) of the numerical solutions obtained with DSMC (left plot) and SWPM (right plot) on the interval $x_2 \in [0.005, 0.6]$. We see very good agreement of the numerical solutions in the “high” density region for both methods. In Fig. 13 we show the same values in the “low” density region $x_2 \in [0.88, 0.995]$. Here we can see that the results obtained using DSMC are reasonable but the confidence bands of SWPM are better. Thus some reduction of the variance is achieved using weighted particles. The relative accuracy (i.e. the quotient of the thickness of the confidence bands and of the exact solution) is presented in Fig. 14. Thus the DSMC scheme is slightly better in the “high” density region and SWPM accuracy becomes much higher in the “low” density region, i.e. for $x_2 > 0.8$. Now we choose the inflow Mach number equal to 7.0 and show the results in the subsequent Figs. 15–17. In the “low” density region we see only some fluctuations obtained using DSMC while the confidence bands for SWPM are still good. Thus an enormous reduction of the variance is achieved using weighted particles. Note that the plot for the relative accuracy is restricted to the interval $x_2 \in [0.005, 0.8]$ because the DSMC results do not allow one a stable computation of the confidence bands behind this point. Thus the DSMC scheme is again slightly better in the “high” density region while it becomes unacceptable for $x_2 > 0.8$. In the next Fig. 18 we show the results for Mach number equal to 10.0 in the “low” density region $x_2 \in [0.88, 0.995]$ only for SWPM. The DSMC results were identical to zero there. The confidence bands of SWPM is still rather good. Thus we have illustrated how

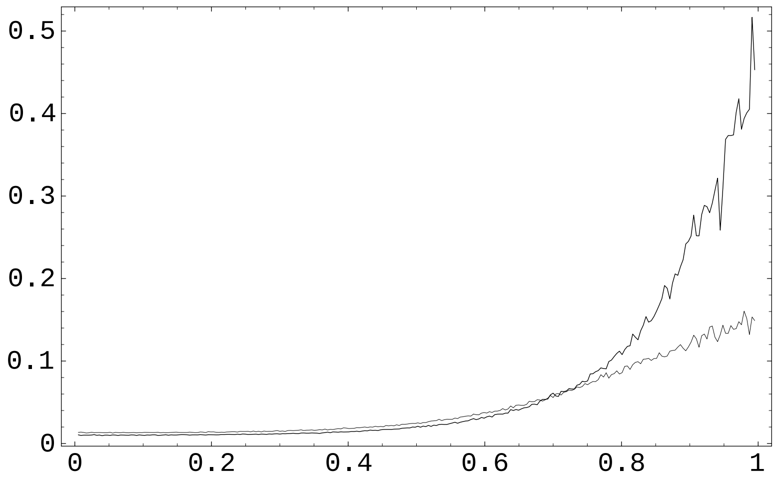

Figure 14: The relative accuracy, $Mach = 5.0$

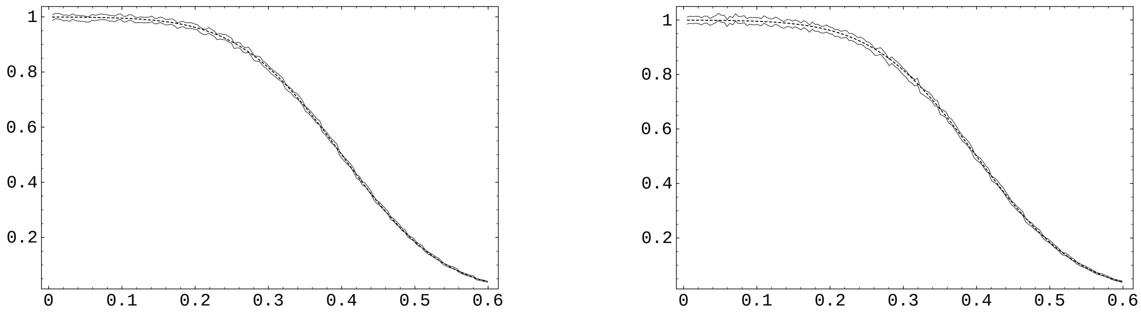

Figure 15: “High” density region, $Mach = 7.0$

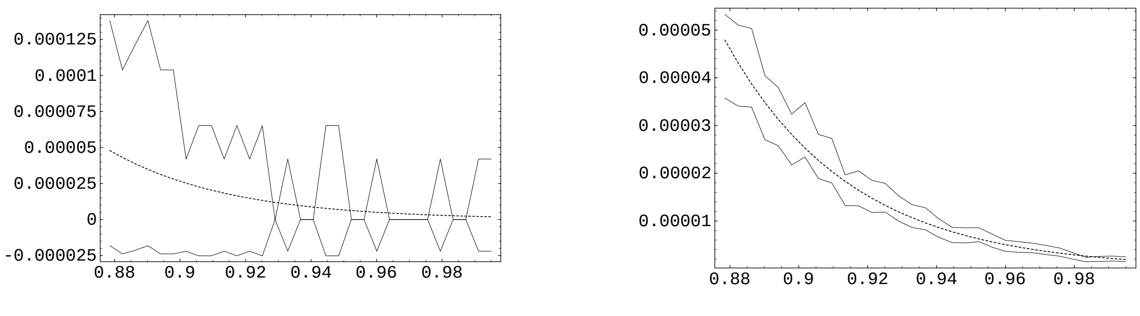

Figure 16: “Low” density region, $Mach = 7.0$

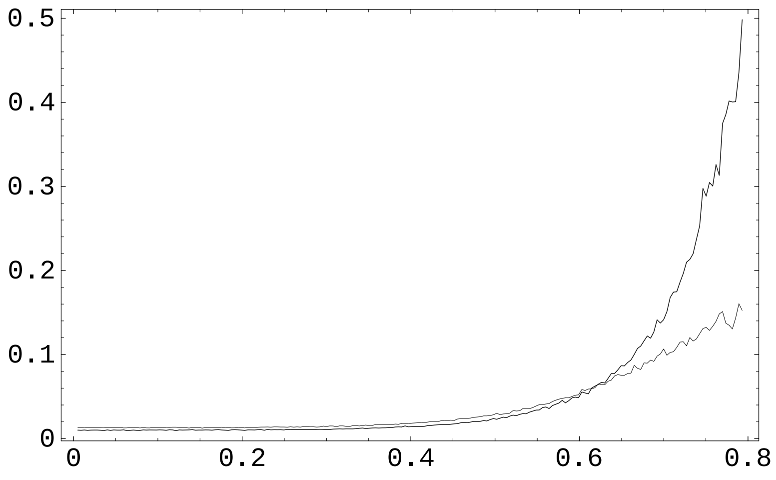

Figure 17: The relative accuracy, $Mach = 7.0$

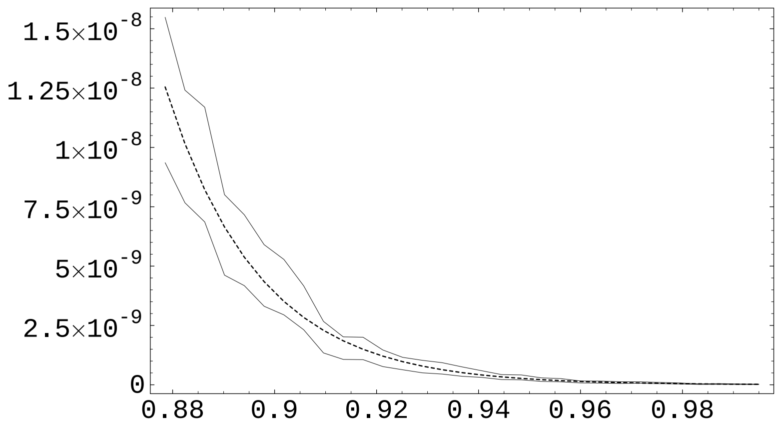

Figure 18: "Low" density region, $Mach = 10.0$

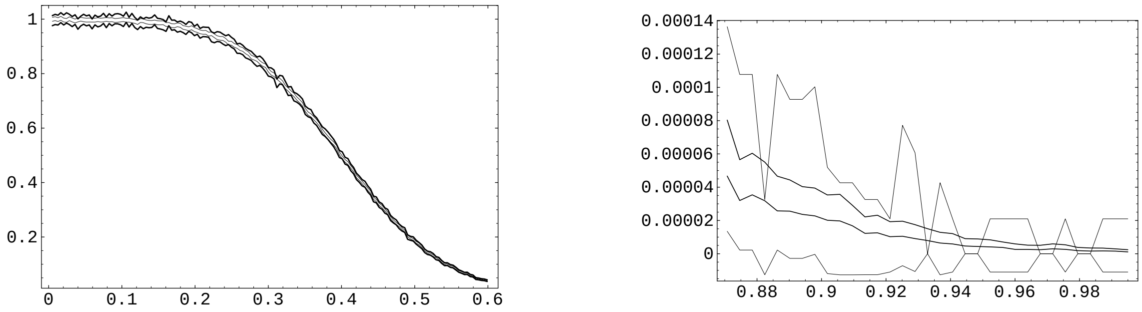

Figure 19: The course of the density, $Mach = 7$

an extremely low density can be resolved using weighted particles.

There is no analytic information in the presence of collisions. Thus in the last Fig. 19 we show only the confidence bands of DSMC (thin lines) and of SWPM (thick lines) for Mach number equal to 7.0 and for Knudsen number equal to 0.1 (c.f. (6)).

The left plot shows the situation in the "high" density region $x_2 \in [0.005, 0.6]$. The low density region $x_2 \in [0.88, 0.995]$ is presented in the right plot. The results were obtained using 1 000 smoothing steps. The number of particles in the DSMC computation was 200 in spatial cells having density 1.0 . The corresponding number was 50 for SWPM having in mind that the number of particles will increases during the collision simulation step. The computational time for SWPM was about a half of the DSMC time. Thus we see a considerable advantage of SWPM when computing small functionals.

The spatial distribution of particles within the computational domain

$$\Omega = (0.0, 2.0) \times (-1.0, 1.0)$$

can be seen in next Figs. 20–21. The first figure shows 25% randomly chosen particles for DSMC (left plot) and for SWPM (right plot) for Mach number equal to 5 while the second figure demonstrates those particles for Mach number equal to 10. The thick solid vertical line indicates in these pictures the line (77).

The effect of better resolution in the physical space due to a better resolution in the velocity space can be clearly seen for SWPM and for Mach number equal to 10 in Fig. 21 while for Mach number equal to 5 the situation is rather similar.

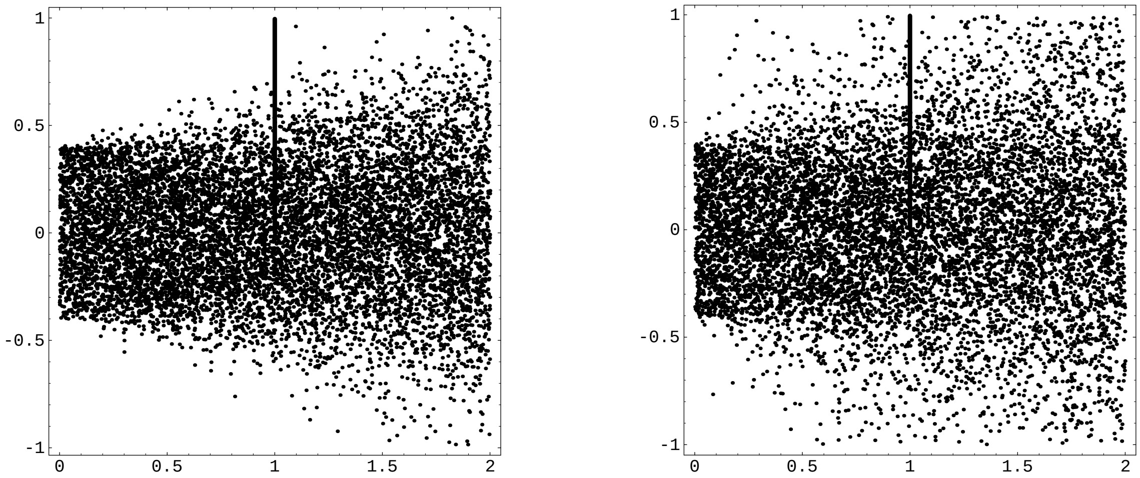

Figure 20: Particles within the computational domain, $Mach = 5.0$

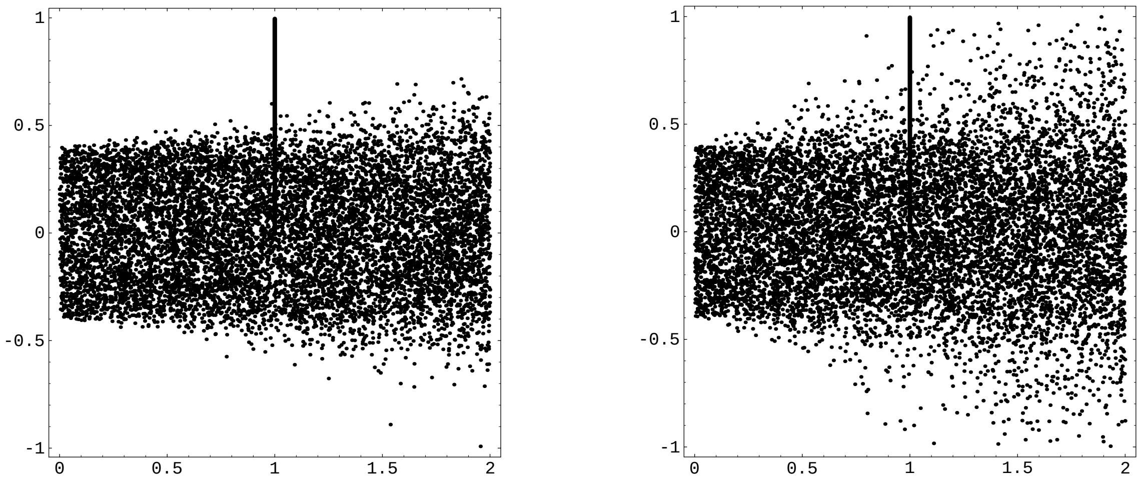

Figure 21: Particles within the computational domain, $Mach = 10.0$

References

[Bir94] G. A. Bird. *Molecular Gas Dynamics and the Direct Simulation of Gas Flows.* Clarendon Press, Oxford, 1994.

[Bob75] A. V. Bobylev. Fourier transform method in the theory of the Boltzmann equation for Maxwell molecules. *Doklady Akad. Nauk SSSR*, 225 : 1041–1044, 1975.

[CIP94] C. Cercignani, R. Illner, and M. Pulvirenti. *The Mathematical Theory of Dilute Gases.* Springer, New York, 1994.

[IR89] M. S. Ivanov and S. V. Rogazinskiĭ. Efficient schemes for direct statistical modeling of rarefied gas flows. *Mat. Model.*, 1(7):130–145, 1989.

[KW77] M. Krook and T.T. Wu. Exact solutions of Boltzmann equation. *Phys. Fluids*, 20(10), 1977.

[MW02] I. Matheis and W. Wagner. Convergence of the weighted stochastic method for the Boltzmann equation. *SIAM J. Sci. Comput.*, 24(5):1589–1609, 2002.

[NGS91] H. Neunzert, F. Gropengiesser, and J. Struckmeier. Computational methods for the Boltzmann equation. In *Applied and industrial mathematics (Venice, 1989)*, pages 111–140. Kluwer Acad. Publ., Dordrecht, 1991.

[RSW98] S. Rjasanow, T. Schreiber, and W. Wagner. Reduction of the number of particles in the Stochastic Weighted Particle Method for the Boltzmann equation. *J. Comput. Phys.*, 145(1) :382–405, 1998.

[RW96a] S. Rjasanow and W. Wagner. Numerical study of a Stochastic Weighted Particle Method for a model kinetic equation. *J. Comp. Phys.*, 128(1) : 351–362, 1996.

[RW96b] S. Rjasanow and W. Wagner. A stochastic weighted particle method for the Boltzmann equation. *J. Comp. Phys.*, 124 : 243–253, 1996.

[RW98] S. Rjasanow and W. Wagner. A generalised collision mechanism for stochastic particle schemes approximating Boltzmann type equations. *Computers Math. Applic.*, 35(1/2) : 165–178, 1998.

[RW01] S. Rjasanow and W. Wagner. Simulation of rare events by the stochastic weighted particle method for the Boltzmann equation. *Math. Comput. Modelling*, 33(8-9):907–926, 2001.

[Sch93] M. Schreiner. Weighted particles in the finite pointset method. *Transport Theory Statist. Phys.*, 22:793–817, 1993.